Study of Dynamic Stress and Life Estimation for Viscoelastic Rotor-A Finite Element Approach

A thesis submitted to National Institute of Technology, Rourkela in partial fulfilment for the degree of

Master of Technology
in
Mechanical Engineering

by

Abhinav Khare
212ME1276

Department of Mechanical Engineering
National Institute of Technology, Rourkela
Rourkela - 769008, Odisha, India
June - 2014

Study of Dynamic Stress and Life Estimation for Viscoelastic Rotor-A Finite Element Approach

A thesis submitted to National Institute of Technology, Rourkela in partial fulfilment for the degree of

Master of Technology
in
Mechanical Engineering
by

Abhinav Khare
212ME1276

Under the guidance of

Dr. H. Roy
Assistant Professor

Department of Mechanical Engineering
National Institute of Technology, Rourkela
Rourkela - 769008, Odisha, India
June - 2014

National Institute of Technology, Rourkela

CERTIFICATE

This is to certify that the thesis entitled, "**Study of Dynamic Stress and Estimation of Life for Viscoelastic Rotor-A Finite Element Approach**", which is submitted by **Mr. Abhinav Khare** in partial fulfilment of the requirement for the award of degree of M.Tech in Mechanical Engineering to **National Institute of Technology, Rourkela** is a record of candidate's own work carried out by him under my supervision. The matter embodied in this thesis is original and has not been used for the award of any other degree.

Dr. H. Roy

Date: Assistant Professor
Place: Rourkela Mechanical Engineering Department

ACKNOWLEDGEMENTS

I am grateful to my supervisor Dr. Haraprasad Roy, whose valuable advice, interest and patience made this work a truly rewarding experience on so many levels. I am also thankful to my friends and colleagues for standing by me during the past difficult times. Particularly, I am indebted to Mr. Saurabh Chandraker for his utterly selfless help.

As for Yogesh Verma , Ranjan Kr. Behra, Rohit Kr. Singh, Abdul Hussian,Naveen Tatapudi ,Mahesh Pol, Aniket Devekar: You were there for me when really needed and I am yours forever.

Abhinav Khare

ABSTRACT

Inherent material damping causes energy dissipation alongside energy storage is predominant phenomenon of viscoelastic material under dynamic loading. For this reason viscoelastic materials are extensively used for vibration control and stability problems. Firstly this work deals with the analytical study of stress developed in viscoelastic beam. Instantaneous stress is obtained by operating instantaneous strain. Modelling technique as ATF (Augmenting Thermodynamic Fields) displacements is used to represent the constitutive relationship in time domain by using certain viscoelastic parameters. This operator based constitutive relationship is used to bring the equations of motion. Finite element technique is used to discretize the continuum by using Euler Bernoulli Beam theory and study has been done for various cases of beams by applying different boundary conditions, under different loading situation. Time domain solution is calculated through state space representation of equation of motion which is further utilized for getting the dynamic stress.

Further this study has been extended to develop a finite element mathematical model of internally damped viscoelastic rotor which is subjected to combined loading (i.e. due to bending and torsion) and also exposed to thermal environment. The shaft damping is incorporated by considering Kelvin – Voigt model. The bending stress & shear stress are calculated along various location as well as different instant of the rotor. Maximum stress location decides the failure point have also been calculated for our further design. Safe design of rotor parameters have been predicted by comparing failure stresses of the system with the Goodman diagram. Our thematic aim was to investigate fatigue behaviour and estimation of rotor life with the help of the S-N curve, which necessitate the calculation of endurance strength that can also be interpolated through Goodman diagram. Numerical results show that the life of the rotor is affected by the temperature but innocent with the axial torque in operating range. It has been concluded through the resultant stresses the design is safe and hence rotor has infinite life of operation.

NOMENCLATURE

l_e	**Length of an Element**
L	**Length of Beam or Shaft**
D_R	**Diameter of Rotor Shaft**
D_D	**Outer Diameter of a Disc**
t_D	**Thickness of Disc**
U	**Unbalance of the Disc**
R	**Position Vector of Displaced Centre of Rotation**
$\bar{y}$	**Lateral Distance from Neutral Axis of Shaft**
y	**Deflection in Lateral Direction**
A	**Area of Cross-Section**
t	**Time**
q	**Nodal Displacement Vector**
I	**Moment of Inertia of Rotor shaft**
E	**Young's Modulus of Elasticity**
ε	**Linear Strain**
$\dot{\varepsilon}$	**Strain Rate**
σ	**Bending Stress**
M_{yy}, M_{zz}	**Bending Moment about Y and Z Axes**
Ω	**Spin Speed**
ω	**Whirl Speed**

V	**Shear Force**
M	**Bending Moment**
ρ	**Volume Density**
η_v	**Coefficient of Viscous Damping**
$\{F\}$	**External Force Vector**
$[M_T]$	**Translatory Mass Matrix**
$[M_R]$	**Rotary Mass Matrix**
$[M]=[M_T]+[M_R]$	**Total Mass Matrix of an Element**
$[G],[K]$	**Gyroscopic and Stiffness Matrices**
$[K_B]$	**Bending Stiffness Matrix**
$[K_C]$	**Skew Symmetric Circulatory Matrix**
$[K_T]$	**Axial Torque Matrix**
$[K_A]$	**Axial Stiffness Matrix**
$[B]$	**Strain Displacement Matrix**
$[\phi_{xy}]$	**Hermite Shape Function in X-Y Plane**
$[\phi_{zx}]$	**Hermite Shape Function in Z-X Plane**
$[\phi]$	**Shape Function**
v, w	**Displacement in Y and Z Axes**

ψ, θ	**Angle of Rotation about Y and Z Axes**
F_s	**Factor of Safety**
σ_u	**Ultimate Strength**
σ_e	**Endurance Strength**
σ_f	**Failure Stress**
N_f	**Life of Component**
$\tau_{\max}, \tau_{\min}$	**Maximum and Minimum Shear Stress**
$\sigma_{\max}, \sigma_{\min}$	**Maximum and Minimum Bending Stress**
τ_m, τ_a	**Mean and Amplitude Value of Shear Stress**
$\sigma_{\mathrm{m}}, \sigma_a$	**Mean and Amplitude Value of Bending Stress**
$\left(\sigma_{eq}\right)_{\mathrm{m}}, \left(\sigma_{eq}\right)_a$	**Mean and Amplitude Value of Equivalent Stress**
α	**Coefficient of Thermal Expansion**
ΔT	**Temperature Difference**
T_R	**External Torque**
P_A	**Axial Load Due to Thermal Load**
$\overline{T}$	**Average Temperature over Cross-Section**
T_O	**Reference Temperature**
ξ	**Augmenting Thermodynamic Field**
H	**Affinity**

b	**Inverse of Relaxation Time**
δ	**Strength of Coupling between Mechanical Displacement Field an Thermodynamic Field**
γ	**Material Property Relating the Changes in** H to ξ

CONTENTS

LIST OF FIGURES

Chapter 1

INTRODUCTION

1.1 Background and Importance

A rotor is considered as long slender one dimensional structure, is mounted by one or more number of bearings through which it can rotate. Earlier it was considered as single mass in the form of a point mass, a rigid disc or a long rigid shaft. Rotating machines ranging from very large systems like power plant rotors, for example, a turbo generator, ship propeller to very small systems like a tiny dentist's drill, with a variety of rotors such as pumps, compressors, steam turbines, motors, turbo pumps etc. are used as example in process industry. The principal components of a rotor-dynamic system are the shaft or rotor with disk and the bearing and shaft or rotor is the rotating component of the system.

Rotors are the major sources of vibration in most of the machines. As the rotation speed increases, the amplitude of vibration often passes a maximum that is called a critical speed. If the amplitude of vibration at a critical speed is excessive, then catastrophic failure can occur. Another phenomenon occurs quite often in rotating machinery is instability. By and large every material is classed as viscoelastic, because damping exhibit in all kind of materials. The internal damping in the shaft or rotating damping generates a tangential force which proposional to the spin speed. Rotors may develop unstable behaviour after certain spin speed. Due to unstable nature and resonance at critical speed, performance or output of rotor is restricted.

Unlike non rotating structure, the rotor is subjected to repetitive loading. Thus there is a chance of damaging the system before yielding due to fatigue stress develop and rotor life reduces. To overcome those problems or to achieve safe operation of the rotor, it is essential to study of rotor and its dynamics.

1.2 Viscoelasticity

Most of the time engineering material show different behaviour as the pure elastic material and deviates from the Hook's law. This is due to some inheritant property of the material which is known as viscoelasticity. Viscoelasticity, as the name implies, is a property that combines elasticity and viscosity. A material, which is viscoelastic in nature stores and also dissipates energies and therefore the stresses in such materials are not in phase with the strain. For this reason, it is extensively used in various engineering applications for controlling the amplitude of resonant vibrations and modifying wave attenuation and sound transmission properties which helps in increasing structural life through reduction in structural fatigue.

The classical theory of elasticity states that for sufficiently small strains, the stress in an elastic solid is proportional to the instantaneous strain and is independent of the strain rate. In a viscous fluid, according to the theory of hydrodynamics, the stress is proportional to the instantaneous strain rate and is independent of the strain. Viscoelastic materials exhibit solid and fluid behaviour. Such materials include plastics, amorphous, polymers, ceramics, glasses and biomaterials such as muscle. Viscoelastic materials are characterized by constant-stress creep and constant-strain relaxation. The Stress-Strain Curves for a purely elastic and a viscoelastic material are shown in fig.1.

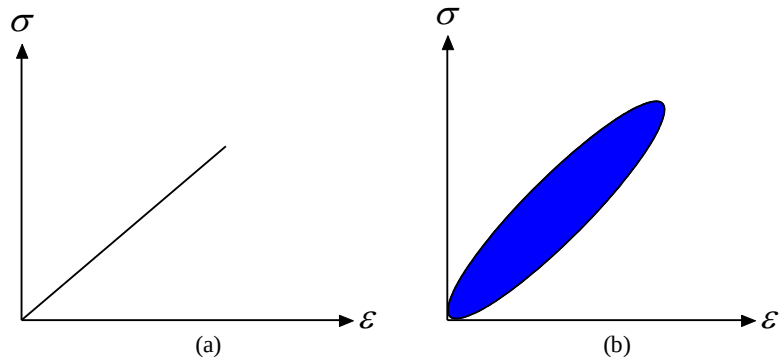

Figure1.1: Stress-Strain Graph for Elastic and Viscoelastic Material

Due to loss of energy during loading and unloading time, the stress strain curve for viscoelastic material is elliptic in nature. The area enclosed by the ellipse is a hysteresis loop and shows the amount of energy lost as heat in a loading and unloading cycle.

The study for rotary machines, requires a careful and detailed analysis, as the rotation movement of the rotor appreciably influences the dynamic comportment of the system, making the modal parameters dependent on the rotation of the machine. The gyroscopic effect couples the rotation movement and, it is dependent on the rotation speed of the rotor. Therefore it is expected that the natural frequencies and vibration modes of a rotating machine also depend on the system speed.

1.3 Dynamic Stress and Fatigue

When load is applied on the body a resistive force set up in the body and this resistive force per unit area of cross section of body is known as stress. The nature of stress depends upon the nature of applied load. In a part subjected to some forces, stresses are generally distributed as a continuously varying function within the continuum of material. Every infinitesimal elements of the material can conceivably experience different stresses at the same time. Normal stresses acts perpendicular (i.e. normal) to the surface of the body and tend to pull it out (i.e. tensile normal stress) or push it in (i.e. compressive normal stress). Shear stresses acts parallel to the surface of the body, in pairs on opposite faces, which tends to distort the cube into a rhomboidal shape. When body is subjected to loads transverse to its length cause body to bend and thus resultant stresses due this type of loading is called bending stress.

Most of the time machine parts are rarely loaded in as simple manner as the specimens used to get the tensile strength. Henceforth if the tensile strengths is taken as design criteria, then they should correlate in some way the actual load which a part is capable of carrying. Component parts such as crankshaft, gears, springs,

shafts, rotor, connecting rod, turbine, etc., are subjected to combined bending and torsion stress as well as to stress repeated in cycles Slaymaker (1959) [1].

There are different types of stresses which a machine components encounters during operation under dynamic loading. (i) The stresses which vary from zero to maximum value are known as repeated stresses. (ii)The stresses which vary from a certain minimum value to a certain maximum value of same nature are known as fluctuating stresses. (iii)The stresses which vary from a minimum value to a maximum of the opposite nature (i.e. from a certain minimum compressive to a certain maximum tensile or from a minimum tensile to a maximum compressive) are known as alternating stresses.

Ductile material include majority of the metals and polymers. Ductile materials have same tensile strength as compressive strength and are not as susceptible to stress raisers as are brittle materials. Two popular theories of yield criteria are presented: the maximum shear stress theory and the distortion energy theory.

Maximum-shear-stress theory was first proposed by Coulomb (1773) but was independently discovered by Tresca (1868) is therefore often called the Tresca yield criterion. This theory states that a part subjected to any combination of loads will fail by yielding or fracture whenever the maximum shear stress exceeds a critical value. The critical value can be determined from standard uniaxial tension tests.

Maximum distortion energy criterion or Von Mises criterion, states that for a given structural material is safe as long as the maximum value of distortion energy per unit volume in that material remains smaller than distortion energy per unit volume required to cause yield in a tensile-test specified of the same material. It is experimentally deduced that distortion energy theory gives best results for ductile material which is subjected to combined loading.

Factor of safety may be defined as a figure used in structural applications that provides a design margin over the theoretical design capacity. It is also known as the

safety factor, it allows for uncertainty in the design process, such as calculations, strength of materials, quality and duty. To ensure good service from a part the condition to which it is subjected should be less severe than the condition which would cause it to fail. Failure occurs when factor of safety becomes less than unity. High stress is generally associated with failure; hence the common conception of factor of safety is ratio of maximum stress to working or design stress.

In fatigue failure most of the failures occurs due to time-varying load rather to static loads. These failures typically occur at stress levels which are significantly lower than the yield strength of the materials. Fluctuating load induce fluctuating or cyclic stress that often result in failure by means of cumulative damage. Fatigue failure is the single largest cause in metals estimated to be 90% of all metallic failures as stated by Bernard (2004) [2]. Fatigue failure are catastrophic and insidious, occurring suddenly and often without warning. Fatigue failure is applicable on both microscopic and macroscopic scales. Fatigue is a complex phenomenon. It is crack propagation, initially on a micro scale and then extremely rapid as the fatigue crack reaches a critical length. Fatigue is concerned whenever cyclic stress are present. Through experiments it has been concluded that fatigue crack generally begins at the surface and propagate through the bulk, unless large subsurface flaws or stress raiser exits in the substrate.

The fatigue or endurance limit of a material is defined as the maximum amplitude of completely reversed bending stress that the standard specimen can withstand for an unlimited number of cycles (10^6 -10^7) without fatigue failure or appearance of crack. For loading other than reversed bending load it known as endurance strength.

Fatigue life is defined as the number of stress cycles that the standard specimen can complete during the test before the appearance of the first fatigue crack. Based on the number of stress cycle that the part is expected to undergo in its lifetime, fatigue is classified as either low cycle fatigue which is generally below 10^3

stress cycles and high cycle fatigue which is generally above 10^3 but less than 10^6 cycles Khurmi and Gupta (2009) [3],Bhandari (2010) [4]. For determination of life of a component, stress-life approach has been employed. This method is the oldest one and used for high cycle fatigue where assembly is expected to last for more than about 10^3 cycles of stress. In this method stress in the system are determined and these stress value are plotted on S-N diagram also called Wohler diagram in order to get life of a machine component corresponding to failure stress in the system. It is best when the load is predictable and consistent over the life of the part as in Norton (2003) [5]. It is a stress-based model, which seeks to determine a fatigue strength or endurance limit for the material so that the cyclic stress can be kept below that level and failure can be avoided for the required number of cycles. The part is then designed based on the fatigue strength or endurance limit of the material and factor of safety.

1.4 Overview of Available Literature

1.4.1 History

The present day requirement for ever-increasing reliability in the field of rotor dynamics is now more important than before and continues to grow constantly. Advances are continually being made in this area, due to the consistent demand from the power-generation and transportation industries. Because of progress made in engineering and materials science, rotatory machinery is becoming faster and lighter, as well as being required to run for longer period of time. All of these factors mean that the direction, location and analysis of faults play a vital role in the field of rotor dynamics.

The rotor-bearing system of modern rotating machines constitutes a complex dynamic system. The modelling of rotors and their associated support structures has been developed to a high degree of sophistication over the past twenty years especially by the use of finite element analysis. The challenging nature of rotor dynamics problems have attracted many scientists and engineers whose

investigations have contributed to the impressive progress in the study of rotating systems. With the advancement in high-speed machinery and increases in their power/weight ratio, the determinations of the rotor dynamic characteristics through reliable mathematical models gains prime importance. The advancement in modern instrumentation and computational capabilities has helped in implementing simulation techniques of these complex models. Modern machinery is bound to fulfil increasing demands concerning durability as well as safety requirements.

Jeffcott (1999) [6] provided a very basic model of a rotor. Initially, he made three assumptions: (i) No damping is associated with the rotor, (ii) Axially Symmetric rotor, and (iii) The rotor carries a point mass. Later, the model was expanded to take care of damping. Although the Jeffcott rotor model is an oversimplification of real-world rotors, it retains some basic characteristics and allows us to gain a qualitative insight into important phenomena typical of rotor dynamics, while being much simpler than more realistic models.

Nelson and McVaugh (1976) [7] written extensively history of rotor dynamics and most of the work is based on Finite Element Methods. There are many software packages that are capable of solving the rotor dynamic system of equations. Rotor dynamic specific codes are more versatile for design purposes. These codes make it easy to add bearing coefficients, side loads, and many other items.

To reduce the vibration problems in the high strength heavy rotors, researcher focused to use the light weight and damped material rotors in spite of using the heavy rotors. This make another revolution in the field of rotor dynamics, through this not only the size of the heavy machine reduces as well as the new concept of using the damped material like viscoelastic are predominant in rotor dynamics. Voigt model (2-element model) was used to represent the shaft material constitutive relationship by Zorzi and Nelson (1976) [8] who discretized shaft continuum using finite beam elements to derive equations of motion and study dynamic behavior of rotor-shaft systems. Researchers like Dutt and Nakra [14], Gunter [24], Genta [23], and Lalanne

and Ferraris [18], studied the stability of the rotor system with internal damping. They obtained the results in form of Campbell diagrams and decay rate plots. Unbalance response and the threshold spin speed known as Stability Limit of Spin Speed were taken as indices of stability.

1.4.2 Recent Research in the Field of Fatigue Analysis

Gujar (2013) [9] calculated the stress induced in stepped shaft of an Inertia dynamometer. System, forces, torque acting on a shaft are also taken into account. Finite element method is employed for stress analysis. Stress concentration is occurred at the stepped, keyways, shoulders, sharp corners etc. caused fatigue failure of shaft. Due to stress concentration which arises due to various factor results in lowering the endurance limit which has been calculated using Modified Goodman Method. Factor of safety and theoretical number cycles for the shaft before failure is estimated.

Elevator drive shaft has been analyzed for failure by Goksenli (2009) [10]. Failure occurred at the keyway of the shaft due to initiation of crack at the edge of keyway. Forces and torque on the shaft are determined and stresses occurring at the failure surface are calculated. Stress analysis is also carried out by using finite element method (FEM) and the results are compared with the calculated values. Endurance limit and fatigue safety factor is calculated using Goodman diagram, fatigue cycle of the shaft is estimated through Wohler diagram. Fracture failure results due to low radius of curvature.

Mahesh (2013) [11] studied the crankshaft for estimation of life through FEM and for this purpose it was necessary to calculate dynamic load, stresses in the system. Finite element analysis is performed on forged steel crankshaft of four stroke engines to obtain the variation of stress magnitude at critical locations. The dynamic force analysis is carried out analytically using MATLAB program, FE model in ANSYS, and boundary conditions are applied according to the engine mounting conditions. The analysis is carried out for different engine speeds and at different

ratio of fillet radius to diameter of crank pin which gives the critical location on the crankshaft. Analysis has been done to calculate fatigue life using stress-cycle(S-N) approach of crankshaft under complex loading conditions. Due to the repeated bending and twisting, results in fatigue as the cracks form in the fillet area.

During operation of rotor the effect of axial torque effect on lateral dynamics has to be taken into account. Therefore Zorzi and Nelson (1977) [25] simulated a finite element model to study the effect of constant axial torque on the dynamics of rotor bearing system. Formulating finite element equation of motion which includes axial torque gives rise to an incremental torsional stiffness matrix. This matrix is circulatory due to non-conservative nature of system.

A stress analysis method for web-core sandwich beams was carried out by Jani et al. [12]. The beam is a transverse cut from a sandwich plate. The structural analysis of the homogenized beam follows thick face plate kinematics giving the deflection, bending moment and shear force distributions. Then the normal stress components can be calculated accurately by reconsidering the periodic structure of the beam. An analytical elastic–plastic stress analysis was done on the metal-matrix composite by Onur and Unrau [13].

A time domain solution is achieved by Roy et al. (2009) [15] using two different displacement modelling techniques namely ATF (Augmenting Thermodynamics Fields) and ADF (Anelastic Displacement Fields) which uses certain viscoelastic parameters. Constitutive relationship are used to obtain equation of motion of the continuum after discretizing it with finite beam elements. Study of dynamic behaviour of composite beams and rotors can be done utilizing this method. Unbalance such as shaft bow or mass unbalance etc. in the rotor results in the whirling of rotor shaft and due to the whirling orbits are forms which can be elliptical or circular in nature. Analysis for stresses in the rotor has been done by Muszynska [16] when simultaneous backward and forward whirl occurs at different section of the rotor under influence of mass imbalance and shaft bow imbalance

located in two axial plane. Zhenxing et al. (2013) [20] developed a model that can be applied to study the influence of thermal effect on flexible multi-body dynamics. A concept of absolute nodal coordinate formulation (ANCF) was used to analyze the coupled thermal-structure using Euler-Bernoulli beam model. Space structures such as satellite, etc. are subjected to mechanical, thermal and dynamic loads. Therefore Narashimha et al. (2010) [21] simultaneously solve heat transfer and structural problem by combining structural displacement and distribution of temperature and with this temperature distribution thermal moment was evaluated. The stiffness of the system changes when it is thermally loaded due to temperature difference and hence this effect is included by Robert D Cook et al. (2002) [22] using finite element method.

1.5 Analysis Objective

In the era of advancement where every care has been taken off to reduce the defects for smooth operation of machinery with low maintenance and for longer life without failure, but there always exists some difference between the actual manufactured machine component and its prototype i.e. manufacturing defect always occurs in each and every product be it due to machining process or may be because of human error etc. In rotor system these inaccuracies may include shaft bow, bearing defects, defects in disk or blades, etc. During assembly or installation of the components of rotor there may occur misalignment between shaft and bearing axis or disc is not line with shaft axis i.e. eccentricity, such type of errors results in unbalance of rotor and the vibrations in the system increases. Eccentricity might result in the overheating at the bearing ends. During operation at high speed these errors cannot be neglected as stress are setup at different section of the rotor which causes instability in the rotor. These stress are dynamic and cyclic in nature which may lead to early failure, so are matter of concern.

It becomes necessary to find stresses arises from various factors as eccentricity, irregularity in material surface, forces, torque, heat generation or eccentric loading etc. Design point must be the highly stressed location in the rotor and analysis must be based on this design point. The nature of stresses plays an important role as in dynamic systems cyclic stresses occurs which are different from static stress and has more detrimental effect. These cyclic stresses causes fatigue in the system which results in catastrophic failure. Thus there is a need to analyze the system for fatigue failure too as it helps to find life of component in terms of revolutions. Catastrophic failure can be prevented by analyzing system for fatigue failure and thus loss which could have been done by this failure can also be saved. Fatigue analysis helps to decide the time for maintenance and therefore ensuring longer life with smoother operation.

1.6 Thesis Outline

Chapter 1 gives a brief introduction of rotor dynamics which is followed by a brief overview of the development of dynamics of rotor shaft systems. It discusses the various rotor models and stability study of systems under various internal and external effects.

Chapter 2 develops the equation of motion for an Euler Bernoulli beam. It discusses the finite element modelling of the system which is later used in the modelling of rotor. It discuss about the bending stresses in beam under dynamic static condition for both undamped and damped beam.

Chapter 3 first develops finite element formulation of the internally damped rotor shaft system and then validates the finite element code for the rotor shaft system with the published results which available in the literature. Further this study is for modelling single disc rotor to find cyclic stresses in the system and to finally fatigue analysis of the rotor shaft.

Finally, in chapter 4, the conclusions, future scope of the work and references along with appendix are included.

Chapter 2

DYNAMICS OF BEAMS

This chapter gives the detailed study of beam. Equation of motion is derived for elastic beam using Euler Bernoulli Beam theory and afterward damping is incorporated through ATF (Augmenting Thermodynamic Field) technique. Initially an undamped beam model is taken and mode shape and frequency response are plotted. Further, equations of motion are used to obtain state space form to find time domain solution. Normal strain and bending stress are determined with the help of these time domain response. Similar study is done for damped system as for undamped system.

2.1 Introduction

A beam can be defined as a structure having one of its dimensions much larger than the other two. The axis of the beams is defined along that longer dimension and cross section normal to the axis is assumed to smoothly vary along the span or length of the beam. Engineering structures often consists of an assembly or grid of beams with cross sections having shapes such as I's or T's. A large number of machine parts also are beam like structures: lever arms, shaft, turbines, ship propeller and quite a lot of aeronautical structures such as wings.

The solid mechanics theory of beams, commonly referred to as 'beam theory' which plays an important role in structural analysis because it provides the designer with simple tool to analyze innumerable structures. Although more sophisticated tools, such as the finite element method etc., are now widely available for the stress analysis of complex structures or beams models, are often used as pre design stage because they provide valuable insight into the behaviour of structures. Such calculations are also quite useful for validating computational solution.

Several beam theories have been developed based on various assumptions, and lead to different levels of accuracy. One of the simplest and most useful of these theories was first given by Euler and Bernoulli and is commonly called as Euler-Bernoulli beam theory. A fundamental assumption of this theory is that the cross section of the beam is infinitely rigid in its own plane, i.e. no deformation occurs in the plane of the cross section. Consequently, in the plane displacement field can be represented by two rigid body translation and one body rotation as in Bauchau and Craig [17]. Two additional assumption deals only with in-plane displacement of the cross-section: during deformation, the cross section is assumed to remain plane and normal to the deformation axis of the beam.

Another beam theory developed is Timoshenko beam theory and it was developed Stephen Timoshenko in the early 20^{th} century. The modal takes into account shear deformation and rotational inertia effects, making it suitable for describing the behavior of short beams, sandwich beams or beams subjected to high-frequency excitation when the wavelength approaches the thickness of the beam.

2.2 Equation of Motion of Undamped Euler Bernoulli Beam

A beam element is shown in fig. 2.1 which subjected to moment and shear force along with the external force. The equation of motion has been derived using Euler-Bernoulli beam theory and by applying force balance and moment balance along the axis of the beam.

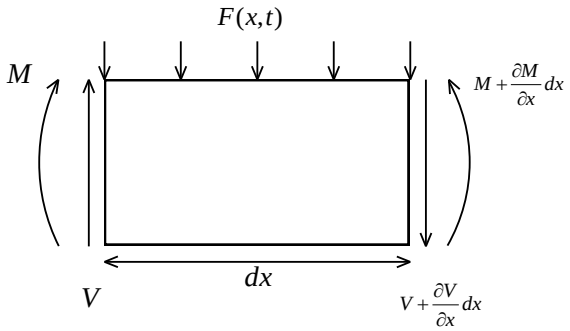

Figure 2.1: Schematic diagram of Euler Bernoulli Beam Section

Now applying force equilibrium on beam section

$$\sum F_x = 0$$

$$\left(\mathrm{V} + \frac{\partial \mathrm{V}}{\partial x} dx\right) - \mathrm{V} + F dx = \rho A \frac{\partial^2 y}{\partial t^2} dx \tag{2.1}$$

$$\frac{\partial V}{\partial x} dx + F dx = \rho A \frac{\partial^2 y}{\partial t^2} dx$$

Simplifying and rearranging the above equation

$$\frac{\partial V}{\partial x} - \rho A \frac{\partial^2 y}{\partial t^2} = -F \tag{2.2}$$

Now applying moment equilibrium on beam

$$\sum M_x = 0$$

$$\left(M + \frac{\partial M}{\partial x} dx\right) - M + V dx + F \frac{dx}{2} dx = 0 \tag{2.3}$$

$$\frac{\partial M}{\partial x} dx + F \frac{dx}{2} dx - V dx = 0 \tag{2.4}$$

In above equation the term $\frac{dx}{2}$ is negligible. Simplifying eq. (2.4) we get

$$V = \frac{\partial M}{\partial x} \tag{2.5}$$

According to beam theory, the bending moment can be written as

$$M = -E I \frac{\partial^2 y}{\partial x^2} \tag{2.6}$$

Then

$$\mathrm{V} = -E I \frac{\partial^3 y}{\partial x^3} \tag{2.7}$$

Differentiating eq. (2.7) w.r.t x

$$\frac{\partial V}{\partial x} = - E\, I \frac{\partial^4 y}{\partial x^4} \tag{2.8}$$

Using eq.(2.8) in eq.(2.2) we get

$$-E\, I \frac{\partial^4 y}{\partial x^4} - \rho A \frac{\partial^2 y}{\partial t^2} = - F \tag{2.9}$$

Rearranging eq.(9) we get

$$E\, I \frac{\partial^4 y}{\partial x^4} + \rho A \frac{\partial^2 y}{\partial t^2} = F \tag{2.10}$$

Thus, governing equation for free vibration of Euler Bernoulli beam

$$\frac{\partial^2 y}{\partial t^2} + \frac{E\, I}{\rho A} \frac{\partial^4 y}{\partial x^4} = 0$$

2.3 Elastic Beam Finite Element Formulation

The Galerkin residual method is employed in the preceding equation to obtain the finite element form.

$$\int_0^{l_e} [\phi_{xy}]^T \left(EIy'''' + \rho A \ddot{y} \right) dx = 0 \tag{2.11}$$

With *EI* constant, and $(\phi_{xy})_i$ are the usual cubic shape functions, two integration by parts of the fourth-derivative term in eq. (2.11) yields

$$\int_0^{l_e} \left[\phi_{xy} \right]^T y'''' dx = \int_0^{l_e} \left[\phi''_{xy} \right]^T y'' dx + \left[\left[\phi_{xy} \right]^T y''' - \left[\phi'_{xy} \right]^T y'' \right]_0^{l_e} \tag{2.12}$$

Substituting eq. (2.6), (2.7) and eq. (2.12) in eq. (2.11) gives

$$\int_0^{l_e} \left(\left[\phi''_{xy} \right]^T EIy'' + \rho A \left[\phi_{xy} \right]^T \ddot{y} \right) dx = 0 = \left[\left[\phi_{xy} \right]^T V - \left[\phi_{xy} \right]^T M \right]_0^{l_e} \tag{2.13}$$

The term *V* and *M* becomes a part of load vector $\{F\}$

$$\ddot{y} = [\phi_{xy}]\{\ddot{q}\} \quad \text{and} \quad y'' = [\mathrm{B}]\{q\} \quad \text{where} \quad [\mathrm{B}] = [\phi''_{xy}], \tag{2.14}$$

$\{q\} = [v_1 \ \psi_1 \ v_2 \ \psi_2]^T$ and $y'' = [\phi''_{xy}]\{q\}$

Substituting eq. (2.14) in eq. (2.13) and assembling elements, we obtain

$$[k]\{q\}_j + [m]\{\ddot{q}\}_j = \{F\} \tag{2.15}$$

With the element matrix expanded to 'structural size', eq. (2.15) is recognized as the standard equation of motion as

$$[\mathrm{K}]\{q\}_j + [\mathrm{M}]\{\ddot{q}\}_j = \{F\} \tag{2.16}$$

where $[\mathrm{K}]$ and $[\mathrm{M}]$ are respectively the global stiffness and global mass matrix.

2.4 Incorporation of Damping Matrix

The damping is incorporated through a modelling technique namely (ATF) Augmenting Thermodynamic Fields as given in Roy et al. [15]. The mechanical and thermal stress, called as affinity are written as

$$\sigma = E\varepsilon - \delta\xi \tag{2.17}$$

$$\mathrm{H} = \delta\varepsilon - \gamma\xi$$

$\bar{\xi}$ is the value of ξ at equilibrium and is obtained as

$$\delta\varepsilon - \gamma\bar{\xi} = 0$$

$$\bar{\xi} = \frac{\delta\varepsilon}{\gamma} \tag{2.18}$$

$$\dot{\xi} = -b(\xi - \bar{\xi}) \tag{2.19}$$

Using eq. (2.18) in eq. (2.19) and rearranging we get

$$\dot{\xi} + b\xi = \frac{b\delta}{\gamma}\varepsilon \tag{2.20}$$

$$\xi(b + D) = \frac{b\delta}{\gamma}\varepsilon \tag{2.21}$$

Rearranging eq. (2.21) we get

$$\xi = \frac{b\delta/\gamma}{(b+D)}\varepsilon \tag{2.22}$$

Using eq. (2.22) in eq. (2.17), neglecting the term $\frac{D}{b}$, as $b, >> 0$, the constitutive relationship is rewritten as

$$\sigma = (a_o + a_1 D)\varepsilon \Rightarrow E()\varepsilon \tag{2.23}$$

where $a_o = E - \frac{\delta^2}{\gamma}$ and $a_1 = \frac{E}{b}$

Operator based equation is achieved to obtain stress. This operator based approach is further employed as

$$M\ddot{q}+K()q=0 \tag{2.24}$$

where $K() = \frac{E()I}{l_e^{\,3}} \int_0^{l_e} [\phi''_{xy}]^T [\phi''_{xy}] dx$

Solving eq. (2.24) we get equation of motion for damp system, where damping matrix is derived from modifying stiffness matrix, is given as

$$\left[C\right] = \frac{EI}{Bl_e^{\,3}} \int_0^{l_e} \left[\phi''_{xy}\right]^T \left[\phi''_{xy}\right] dx \tag{2.25a}$$

$$\left[K\right] = \frac{I}{l_e^{\,3}} \left(E - \frac{\delta^2}{\gamma}\right) \int_0^{l_e} \left[\phi''_{xy}\right]^T \left[\phi''_{xy}\right] dx \tag{2.25b}$$

Mechanical strain and stress in finite element form is given by eq. (2.26)

$$\in_x \; = \bar{y}\left[\phi''_{xy}\right]^T \{q\}, \tag{2.26a}$$

$$\sigma_x = E\,\bar{y}\left[\phi''_{xy}\right]^T \{q\} \tag{2.26b}$$

2.5 Numerical Problem for Beam

A cantilever beam of rectangular cross section is taken and is discretized into finite elements. Each element has two nodes and four degree of freedom. This beam is symmetric about x-axis and loaded harmonically at its free end. A finite element analysis based on Euler-Bernoulli beam theory has been done to determine the mode shape and frequency response. For this purpose a matlab code is developed to find the eigenvalues, eigenvectors and response pattern. Then bending stress for undamped and damped system is determined using time domain response. The schematic diagram in Fig. 2.2 shows a cantilever beam.

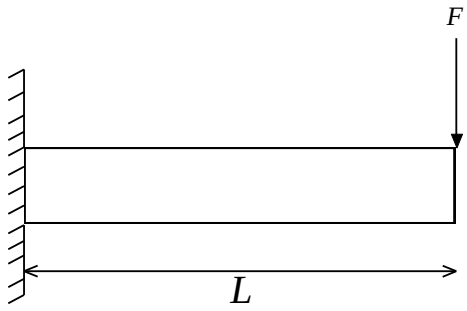

Figure 2.2: Schematic Diagram of Cantilever Beam

Data for the mild steel cantilever beam is density $(\rho) =$ 7800kg/m^3, modulus of Elasticity $(E) = 2\times 10e11$ Pa, amplitude of applied force $(F) =$ 1N, beam length $(L) = 0.6$m, Width= 0.04m, Depth=0.07m

Fig. 2.3 shows first three mode shapes plotted from Eigen vector of undamped beam system. A normal mode of a vibrating or oscillating system is a pattern of motion in which all parts of the system move sinusoidally with the same frequency and with a fixed phase relation.

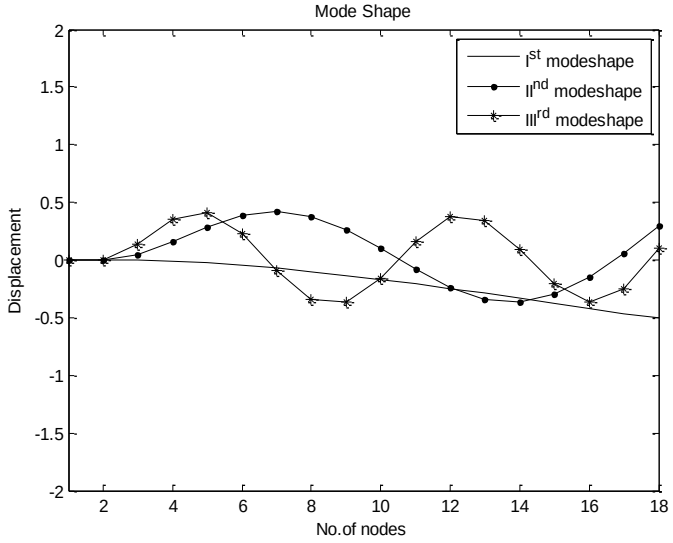

Figure 2.3: Mode shapes of Cantilever Beam

The frequencies of the normal modes of a system are known as its natural frequencies or resonant frequencies and fig. 2.4 shows frequency response of the free end of the beam, when an external cosine function is applied. It is obtained by calculating displacement (response) from equation of motion for different frequency.

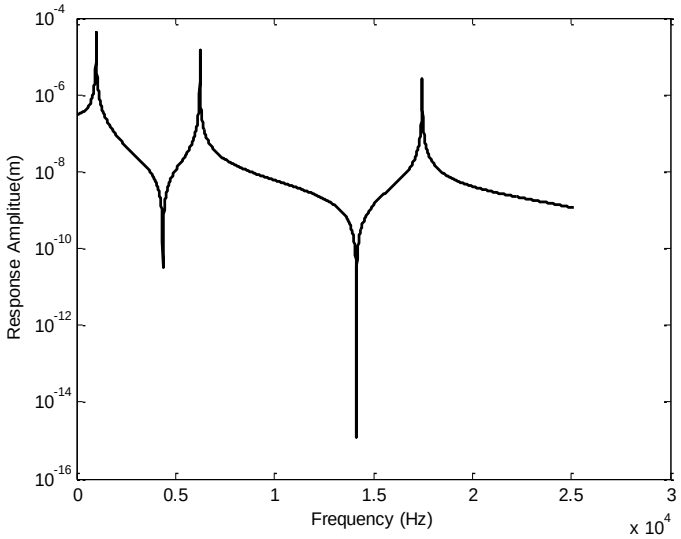

Figure 2.4: Frequency Response at Free End of Beam

Now time dependent response for beam tip is obtained for undamped system by formation of the state space form. Fig.2.5 and Fig.2.6 gives the displacement and stress variation with respect to time for undamped beam and the nature of both the curves are same indicating the steady state fluctuation.

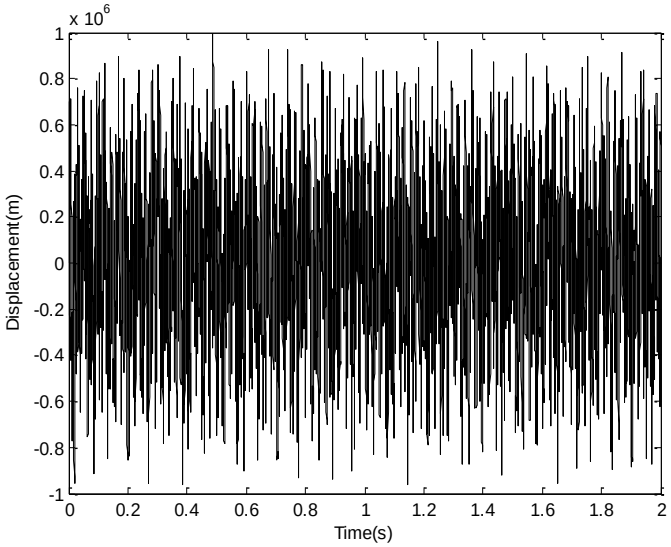

Figure 2.5: Response-Time Plot for Free End of Beam

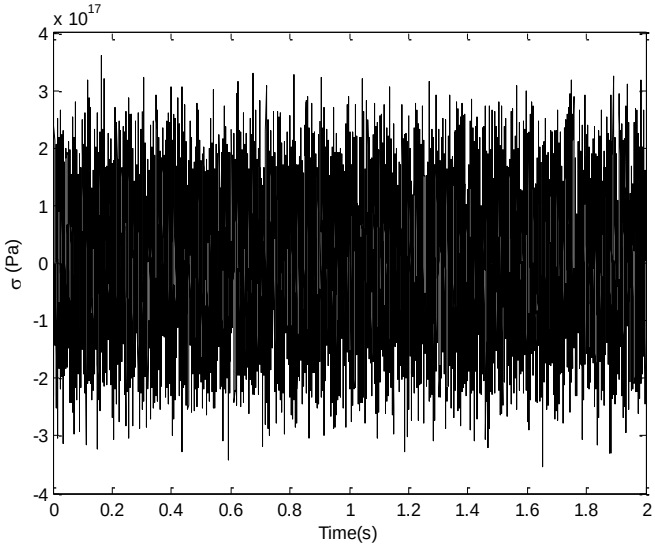

Figure 2.6: Stress-Time Plot for Free End of Beam

Fig. 2.7 shows the stress vs. strain. The plot is a straight line between stress and strain for the cantilever beam and is similar to elastic stress-strain plot.

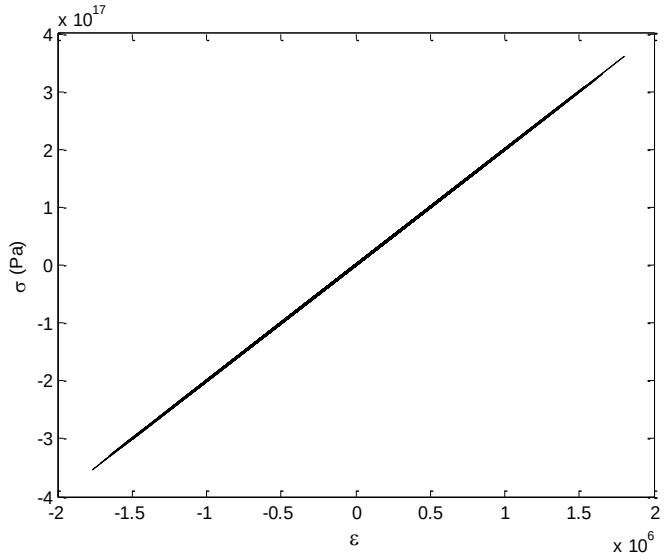

Figure 2.7: Stress-Strain Plot Considering Undamped Beam

Study of undamped system is further extended to damped system and damping is achieved in the system as given section 2.4, where b, γ, and δ are ATF parameters and their values for steel are given in Roy et al. [15] are b = 1.807e5; γ =1.807e5; δ=3.186e7. The response and stress plot for damped system shows the constant amplitude after some time, this shows that the system is under steady state excitation.

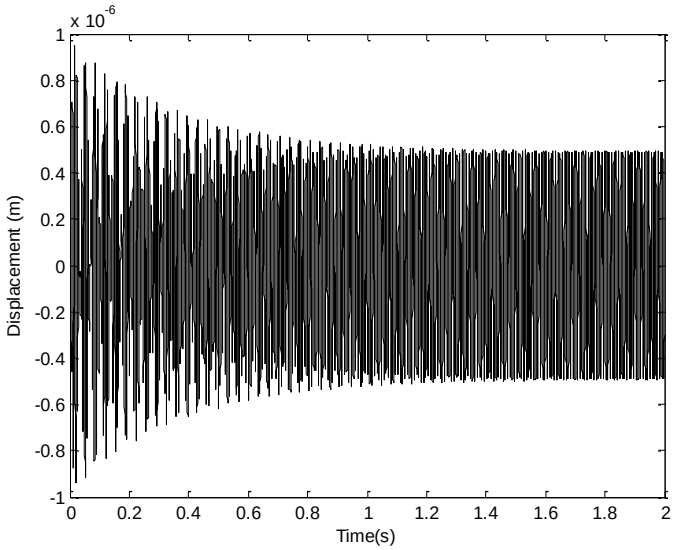

Figure 2.8: Response-Time Plot at Free End of Damped Beam

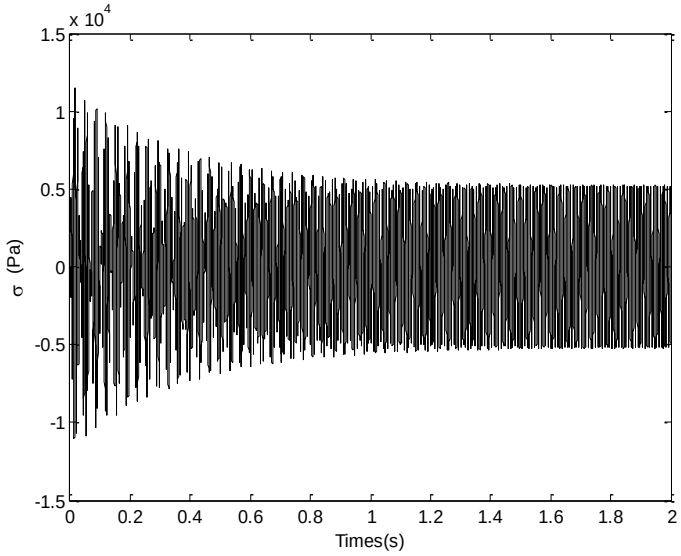

Figure 2.9: Stress-Time Plot at Free End of Damped Beam

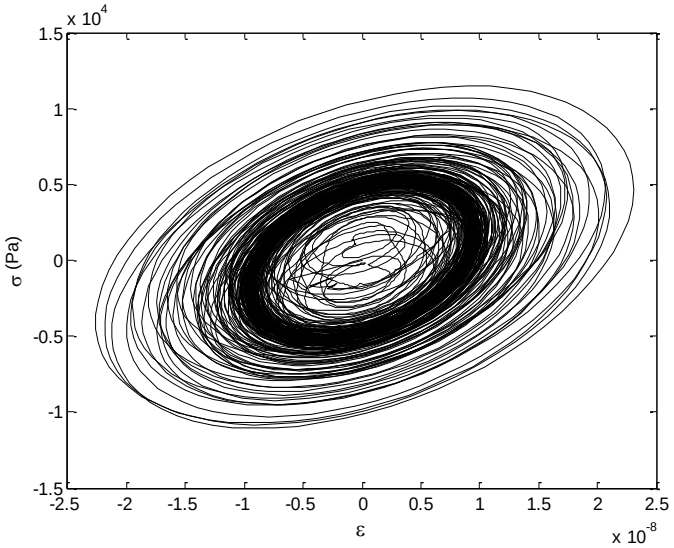

Figure 2.10: Stress-Strain Plot Considering Damped Beam

In undamped system the stress-strain graph in fig 2.7 shows a straight line thus follows hook's law for elastic material. Whereas in damped system, due to energy dissipation stress-strain plot is elliptical nature as shown in fig. 2.10. Therefore results for damped beam or viscoelastic beam are as expected and are in accordance with the theory.

Chapter 3

FATIGUE ANALYSIS OF ROTORS

In this section mathematical formulation of finite element model for rotor is done and the gyroscopic effect due to disc and inertia due to rotation is also taken into account. Formulation for fatigue analysis is also given in this section. The motion is considered in two dimensional plane. The work starts with the validation of finite element code with the published results and further this work is extended for fatigue analysis of single disc rotor system.

3.1 Introduction

A rotor is a body suspended through a set of cylindrical hinges or bearings that allows it to rotate freely about an axis fixed in space. Jeffcott rotor can be stated as the simplest example of rotor which consists of a point mass attached to the massless shaft or the rotor is considered as single mass in the form of a point mass, a rigid disc or a long rigid shaft. Rotors fall into two groups. First one is where the rotor is rigid and does not deflect up to and including the operating speed. The other group comprises flexible rotors that "bow" up to the operating speed.

Rotating shaft are employed in industrial machine such as steam and gas turbines, turbo generators, internal combustion engines, reciprocating and centrifugal compressor or automobile machinery for power transmission. To overcome the ever increasing demand for power and high speed transportation, the rotors of these machines are made extremely flexible, which makes the study of vibratory motion an essential part of design.

3.2 Mathematical Formulation

In this section the mathematical modelling of viscoelastic rotor shaft is represented. The finite element model of the viscoelastic rotor shaft system is based on the Euler-Bernoulli beam theory. The equation of motion is obtained from the constitutive relation where the damped shaft element is assumed to behave as Voigt model i.e., combination of a spring and dashpot in parallel

3.2.1 Finite Element Model

The displaced position of the shaft cross section is shown by fig. 3.1 as in [26]. The displacement of the shaft center along Y and Z direction is indicated by (v, w) and an element of differential radial thickness dr at a distance r (where r varies from 0 to r_o) subtending an angle $d(\Omega t)$ where Ω is the spin speed in rad/sec and Ωt varies from 0 to 2π at any instant of time $'t'$. Due to transverse vibration the shaft is under two types of rotation simultaneously, i.e., spin and whirl ω is the whirl speed.

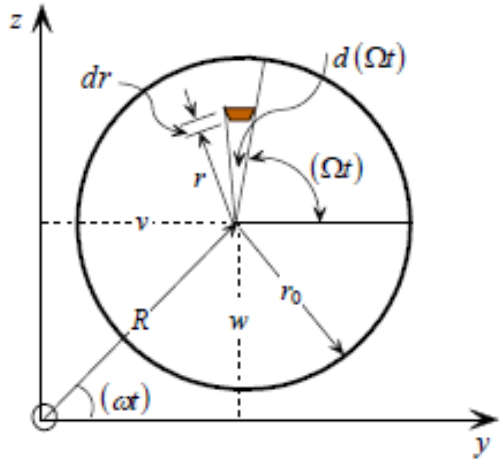

Figure 3.1: Displaced Position of the Shaft Cross - Section

The dynamic longitudinal stress and strain induced in the infinitesimal area are σ_x and ε_x respectively. The expression of σ_x and ε_x at an instant of time are given as Zorzi and Nelson [8].

$$\sigma_x = E\left(\varepsilon+\eta_v\dot{\varepsilon}\right), \quad \varepsilon_x = -r\cos\left[\left(\Omega-\omega\right)t\right]\frac{\partial^2 R(x,t)}{\partial x^2} \tag{3.1}$$

Following [8] the bending moments at any instant of time about the *y* and *z*-axes are expressed as

$$M_{zz} = \int_0^{2\pi}\int_0^{r_0} -\left(v + r\cos\left(\Omega\, t\right)\right)\sigma_x\left(r\, d\, r\right)\, d(\Omega\, t)$$

$$M_{yy} = \int_0^{2\pi}\int_0^{r_0} \left(w + r\sin\left(\Omega\, t\right)\right)\sigma_x\left(r\, d\, r\right)\, d(\Omega\, t) \tag{3.2}$$

After following Zorzi and Nelson [8] and utilizing equation (3.2), the governing differential equation for one shaft element is given as:

$$\left(\left[M_T\right]+\left[M_R\right]\right)\left\{\ddot{q}\right\}+\left(\eta_V\left[K_B\right]+\Omega\left[G\right]\right)\left\{\dot{q}\right\}+\left(\left[K_B\right]+\eta_V\Omega\left[K_C\right]-\left[K_T\right]-\left[K_A\right]\right)\left\{q\right\}=\left[F\right] \tag{3.3}$$

In the preceding equation $\left[M_T\right]$, $\left[M_R\right]$, $\left[G\right]$, $\left[K_B\right]$, $\left[K_C\right]$, $\left[K_T\right]$, $\left[K_A\right]$ are translational mass matrix, rotary inertia matrix, gyroscopic matrix, bending stiffness matrix, skew symmetric circulatory matrix, stiffness matrix due to externally applied torque , axial stiffness matrix due to thermal load respectively. $\left\{q\right\}_{8\times1}$ is the nodal displacement vector and η_V is coefficient of viscous damping. After referring to [25] and [22], $\left[K_T\right]$, $\left[K_A\right]$ are incorporated. It is due to externally applied axial torque and axial elongation for temperature difference between shaft and surrounding. The

matrix expression used in eq. (3.3) are given below following [27]. The elements in the matrices are given in detail in the appendix.

$$\left[M_T\right]=\int_0^{l_e}\rho A\left[\phi(x)\right]\left[\phi(x)\right]^T dx, \qquad \left[M_R\right]=\int_0^{l_e}\rho I\left[\phi'(x)\right]\left[\phi'(x)\right]^T dx$$

$$\left[G\right]=\int_0^{l_e}2\Omega\rho I\left[\phi'(x)\right]\begin{bmatrix}0 & 1\\ -1 & 0\end{bmatrix}\left[\phi'(x)\right]^T dx, \qquad \left[K_B\right]=\int_0^{l_e}EI\left[\phi''(x)\right]\left[\phi''(x)\right]^T dx,$$

$$\left[K_T\right]=\int_0^{l_e}T_A\left[\phi''(x)\right]^T\begin{bmatrix}0 & 1\\ -1 & 0\end{bmatrix}\left[\phi'(x)\right]dx, \qquad \left[K_C\right]=\int_0^{l_e}EI\left[\phi''(x)\right]\begin{bmatrix}0 & 1\\ -1 & 0\end{bmatrix}\left[\phi''(x)\right]^T dx$$

$$\left[K_A\right]=P_A\int_0^{l_e}\left[\phi'(x)\right]\left[\phi'(x)\right]^T dx, \qquad \left\{q\right\}=\left\{v_1 \quad \psi_1 \quad w_1 \quad \theta_1 \quad v_2 \quad \psi_2 \quad w_2 \quad \theta_2\right\}^T, \text{in}$$

which, the Hermite shape function matrix $\left[\phi(x)\right]$, is given by $\left[\phi(x)\right]=\begin{bmatrix}\left\{\phi_{xy}(x)\right\} & \{0\}\\ \{0\} & \left\{\phi_{zx}(x)\right\}\end{bmatrix}$, with subscripts in the elements showing the respective planes.

The axial load due to thermal expansion is given as $P_A=E\alpha\left(\overline{T}-T_O\right)$ where α is coefficient of thermal expansion, $\overline{T}$ is the average temperature over the cross-section and T_O is the reference temperature. T_A is the magnitude of applied external axial torque. ρ is the mass density. A is area of cross-section and I is moment of inertia of shaft. E is the Young's Modulus

3.2.2 Fatigue Analysis

Axial strain and strain rate of the viscoelastic rotor shaft system due to transverse loading in terms of shape function and nodal coordinate can be expressed as

$$\in_x = \overline{y}\left[\phi''(x)\right]^T\{q\}, \quad \dot{\in}_x = \overline{y}\left[\phi''(x)\right]^T\{\dot{q}\} \tag{3.4}$$

where, $\bar{y}$ is the lateral distance from the neutral axis of shaft.

Bending stress develop in the axial direction is given as

$$\sigma_x = E\,\bar{y}\left[\left(\left[\phi''(x)\right]^T\{q\}\right)+\left(\eta_v\left[\phi''(x)\right]^T\{\dot{q}\}\right)\right] \tag{3.5}$$

According to beam theory, bending moment and shear force are written as

$$\frac{M}{I}=\frac{\sigma_x}{\bar{y}},\ \text{and}\ V=\frac{\partial M}{\partial x} \tag{3.6}$$

After utilizing the preceding equation, the shear force for viscoelastic material is given as

$$V = EI\left[\left(\left[\phi'''(x)\right]^T\{q\}\right)+\left(\eta_v\left[\phi'''(x)\right]^T\{\dot{q}\}\right)\right] \tag{3.7}$$

The shaft having circular cross-section, maximum shear stress is given by

$$\tau_{\max}=\tfrac{4}{3}\tau_{avg} \tag{3.8}$$

where average shear stress, $\tau_{avg}=\dfrac{V}{A}$

Endurance strength of the rotor shaft is determined with help of Goodman equation, so for this it is necessary to find mean and amplitude values of bending and shear stress as

$$\sigma_m=\frac{\sigma_{\max}+\sigma_{\min}}{2}\ ,\ \sigma_a=\frac{\sigma_{\max}-\sigma_{\min}}{2} \tag{3.9}$$

Subscript m stands for mean or average value and a is for amplitude or variable value. Similarly mean shear stress τ_m and amplitude shear stress τ_a can be calculated from the shear stress fluctuation. After calculating all stresses from the above relations, equivalent mean stress and equivalent amplitude stress are calculated from distortion energy theory as in reference [5].

$$(\sigma_{eq})_m = \sqrt{(\sigma_m)^2 + 3(\tau_m)^2}\ ,\ (\sigma_{eq})_a = \sqrt{(\sigma_a)^2 + 3(\tau_a)^2} \tag{3.10}$$

And now endurance strength (σ_e) can be determined from Goodman equation as given in eq. (3.11) with some assumed value of factor of safety referring to [10].

$$\frac{(\sigma_{eq})_a}{\sigma_e} + \frac{(\sigma_{eq})_m}{\sigma_u} = \frac{1}{F_s} \tag{3.11}$$

For fatigue analysis the primary condition is to know the value of stress which results in failure and for safe operation of the system the operating stresses must be kept below this failure stress (σ_f). Fig.3.2 shows the Goodman diagram whose ordinate and abscissa indicate the amplitude and mean stress. Goodman line is drawn for interpolation purpose, which is between the ultimate and endurance stress point. The operating stress point *X* is obtained from the coordinate values of $(\sigma_{eq})_m$ and $(\sigma_{eq})_a$. For safe design the point *X* should be below the Goodman line. The failure stress point is achieved by line joining between ultimate stress point to point operating stress point *X* and extending it to ordinate. Thus from this diagram failure stress can be interpolated using similar triangles as given in [11]. Interpolated relation for failure stress is given as follows.

$$\sigma_f = \frac{(\sigma_u)(\sigma_{eq})_a}{(\sigma_u) - (\sigma_{eq})_m} \tag{3.12}$$

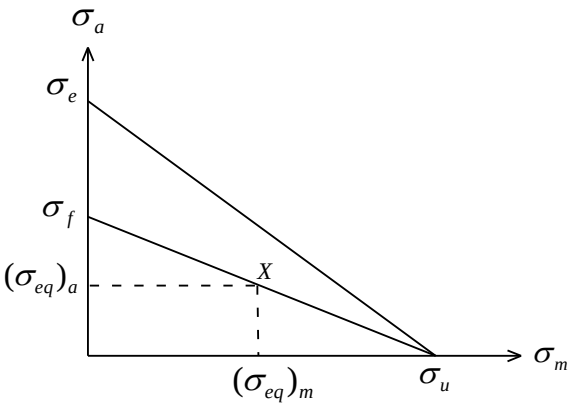

Figure 3.2: Goodman Diagram for Interpolating Endurance Strength

S-N curve also known as Wohler diagram for high cycle fatigue, is shown in fig.3.3, which is the stress vs. operating cycle diagram in logarithmic scale. Life can be determined corresponding to the failure stress (σ_f) through Wohler diagram again by using similarity of triangles and the interpolated relation is

Life $N_f = 10^{\,p}$ (3.13)

where $P = 3 + (6-3)\dfrac{\log(0.9\sigma_u) - \log(\sigma_f)}{\log(0.9\sigma_u) - \log(\sigma_e)}$

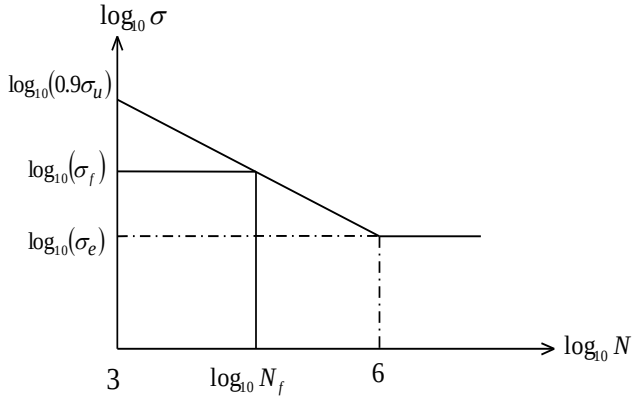

Figure 3.3: Stress-Cycle(S-N) Diagram

3.3 Numerical Problem

3.3.1 Validation of Finite Element Code

The schematic diagram of three disc rotor shaft system is shown in fig. 3.4 as given in Lalanne and Ferraris [18]. A rotating shaft system with simply supported ends is considered without axial load and axial torque i.e. $P_A = 0,\ T_A = 0$. Few numerical results are obtained for validation purpose.

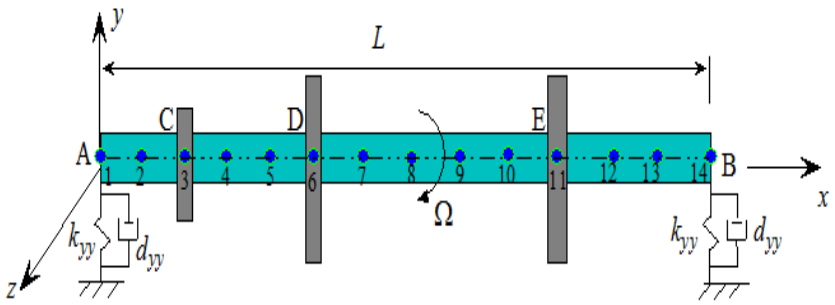

Figure 3.4: Schematic Diagram of Lalanne Rotor

The material properties of the steel rotor are shown in table 3.1 and table 3.2 shows the dimensions and mass unbalance of these three discs. Following Lalanne and Ferraris [18], initially the discs are placed at nodes 3, 6 and 11. The unbalance is considered at disc-2 and it is 200 gm. mm

Material	**Density** (kg/m^3)	**Young's Modulus** (GPa)	**Length** (m)	**Diameter** (m)	**Coefficient of Viscous Damping** (s)
Mild steel	7800	200	1.3	0.2	0

Table 3.1: Rotor Material and its Properties

Disc	**Diameter** (m)	**Thickness** (m)	**Mass Unbalance** (kg-m)
1	0.24	0.05	0
2	0.40	0.05	2×10^{-4}
3	0.40	0.06	0

Table 3.2: Disc Dimensions and Unbalance for Three Disc

The Campbell diagram is plotted in fig. 3.5 which give the critical frequencies of the system. It shows the forward and backward whirl lines and gives the critical frequency when whirl lines are cut by line inclined at 45°, known as synchronous whirl line (SWL). Frequency response plot is shown in fig. 3.6. Peaks in the graph shows the resonance in the system at corresponding frequency i.e. system is unstable at these frequency because frequency of the forcing function coincides with the natural frequency of the system and this condition is called resonance. When the system is under resonance condition large amplitude vibrations takes which may lead to failure and thus system must be avoided to run at critical frequencies to avoid failure.

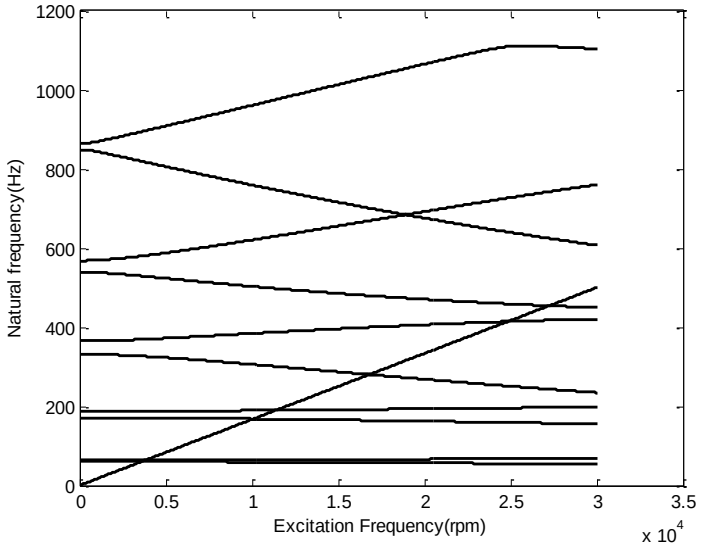

Figure 3.5: Campbell Diagram

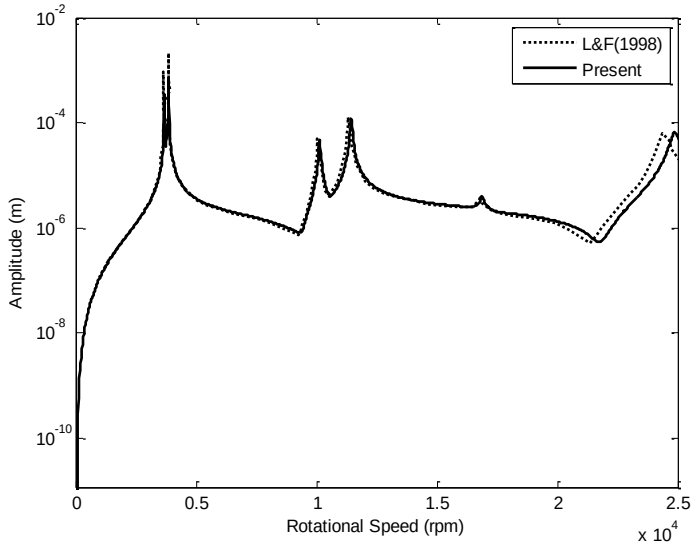

Figure 3.6: Mass Unbalance Response

The eigenvalues and eigenvectors obtained to find out the stability of the system. Close match between the computed and reported results in Lalanne [18] validate the correctness of the code as shown by table below

S. No.	Frequency	Present Result	L&F (1998)
1.	F1	54	55.41
2.	F2	68	67.20
3.	F3	154	157.9
4.	F4	196	193.6
5.	F5	232	249.9
6.	F6	415	407.5
7.	F7	444	446.7
8.	F8	599	714.9
9.	F9	751	622.7
10.	F10	1089	1076

Table 3.3: Frequency Validation

3.3.2 Single Disc Rotor

A rotor shaft system having AISI/SAE 1050 cold drawn steel shaft with simply supported bearing ends with disc at the center is considered which is subjected to thermal load due to temperature difference with the environment and an external axial torque is applied. The bearing is modelled as a flexible damped support having stiffness and damping coefficients (k_{yy}, c_{yy}) and (k_{zz}, c_{zz}) in the *x*-*y* and *x*-*z* planes respectively. The schematic diagram for rotor shaft system is shown in fig. 3.7.

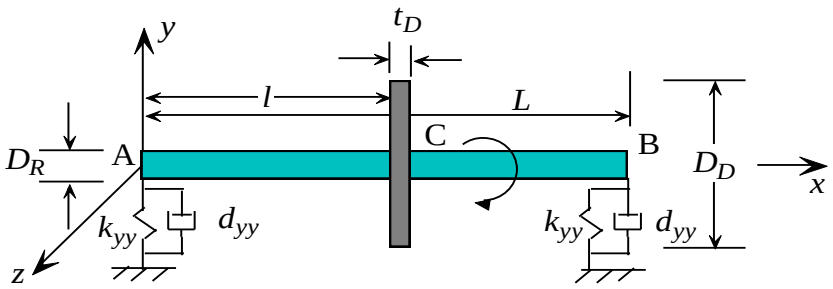

Figure 3.7: Schematic Diagram of Single Disc Rotor

Data for the system are $k_{yy} = k_{zz} = 7e7$ N/m, $c_{yy} = c_{zz} = 7e2$ N/m, Length of rotor is $L = 1.0$ m, diameter of rotor is $D_R = 0.07$ m, diameter and thickness of disc are $D_D =$ 0.4 m, $t_D =$ 0.05 m respectively, and the unbalance of the disc, U = 200 gm-mm. Material property are as follows $E = 2e11$Pa, $\rho = 7850$kg/m^3, $\eta_V = 2e^{-4}$ sec, Ultimate strength of steel $(\sigma_u) =$ 690e6 Pa, Coefficient of thermal expansion $(\alpha) = 13e\text{-}6\ ^\circ\text{K}^{-1}$.

An internally damped rotor shaft with disc at the centre is taken for fatigue analysis. The shaft is discretized into ten elements with disc placed at centre node and the unbalance is considered at disc and it is 2×10^{-4} kg-m.

A MATLAB code is written based on the FE formulation for numerical simulation. The eigen values of the system are determined and the maximum real part of all eigen values are plotted against spin speed, this graph is called decay rate plot as shown in fig. 3.8. It is seen from the plot that the maximum real part increases from negative to positive with spin speed. After certain spin speed it touches zero line and system become unstable. The corresponding spin speed is called stability limit of spin speed.

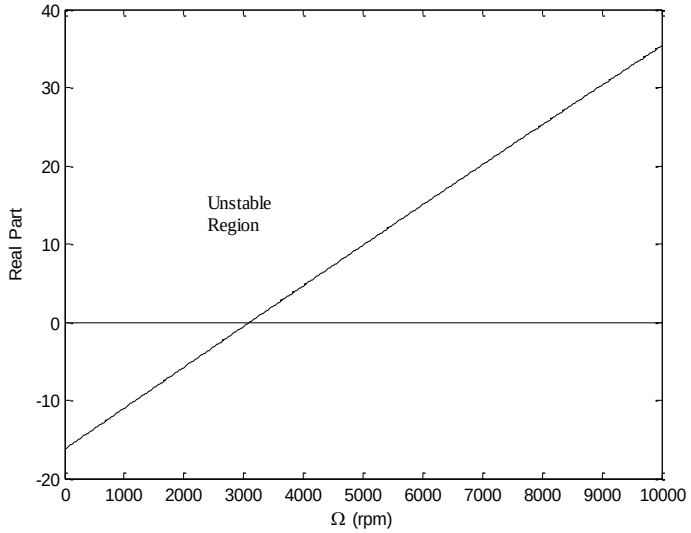

Figure 3.8: Decay Rate Plot

Stability limit of spin speed (SLS) of the rotor shaft system is drawn for various axial torque and various values of temperature difference. The SLS is obtained from the eigenvalues, when all the eigenvalues have negative real part, the system is stable. When the real part touches the zero line, the corresponding spin speed is called SLS. Fig. (3.9 a) shows the SLS vs axial torque, when the temperature is remain constant ($\Delta T = 30^{\circ}$K). The SLS for various values of temperature difference is plotted in fig. (3.9 b) for a constant value of axial torque ($T_A = 1000$N-m). It can be seen that SLS is almost innocent with the increase of torque but decrease with the increase in temperature. With increase in temperature, reduction in system effective stiffness, results to decrease the SLS. Therefore system stresses are found out at spin speed of 3100 rpm with axial torque equal to 1000N-m and at temperature difference of 30° K.

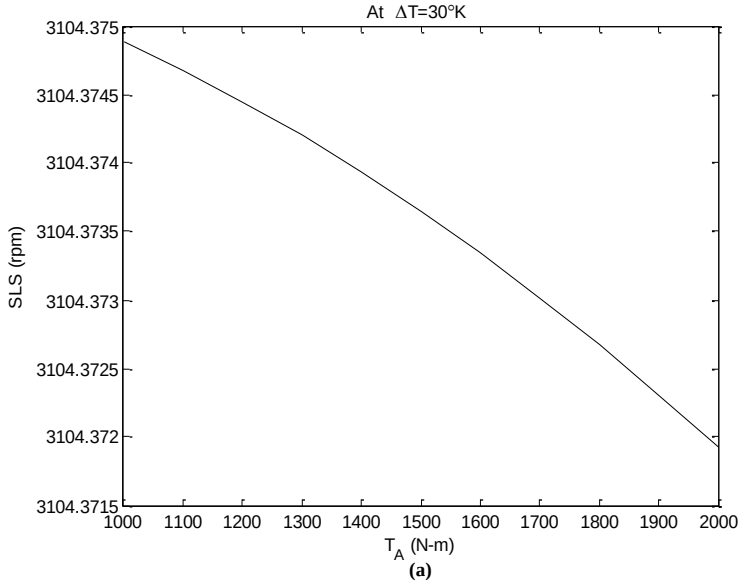

Figure 3.9: SLS for different Axial Torque and Temperature Difference Respectively

Fig. 3.10.(a, b, c) shows the time varying bending stress, shear stress and their equivalent stress for various non-dimensional location denoted as (L*) of the

rotor shaft respectively where 0 and 1 on abscissa denote left hand side and right hand side of shaft respectively.

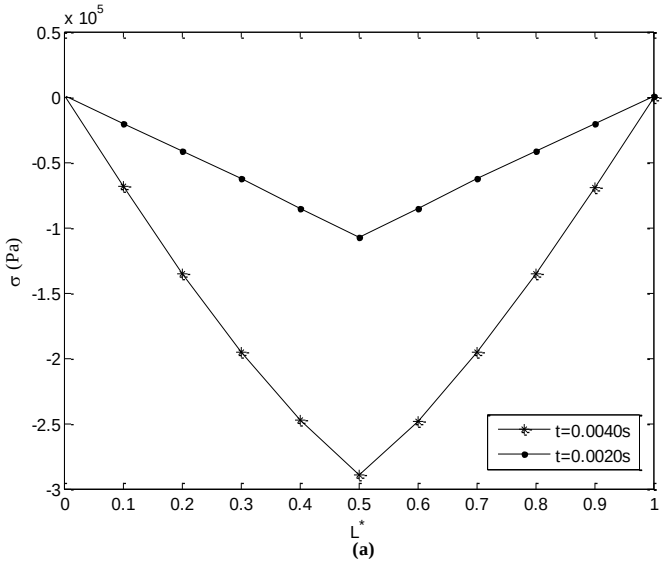

(a)

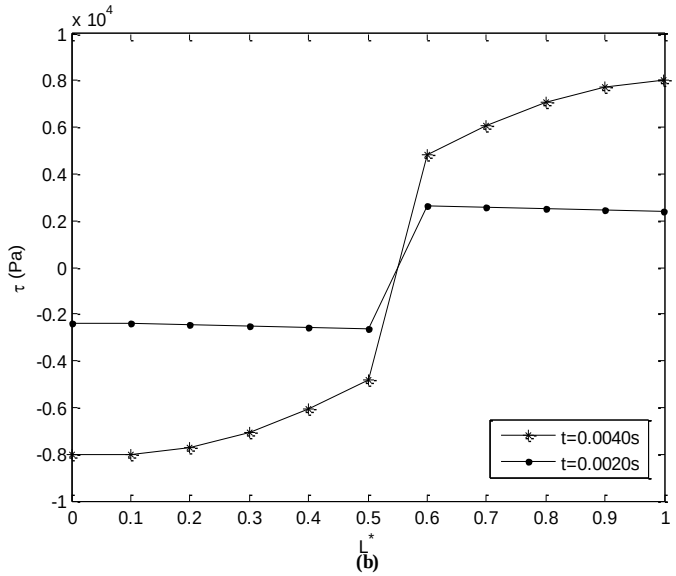

(b)

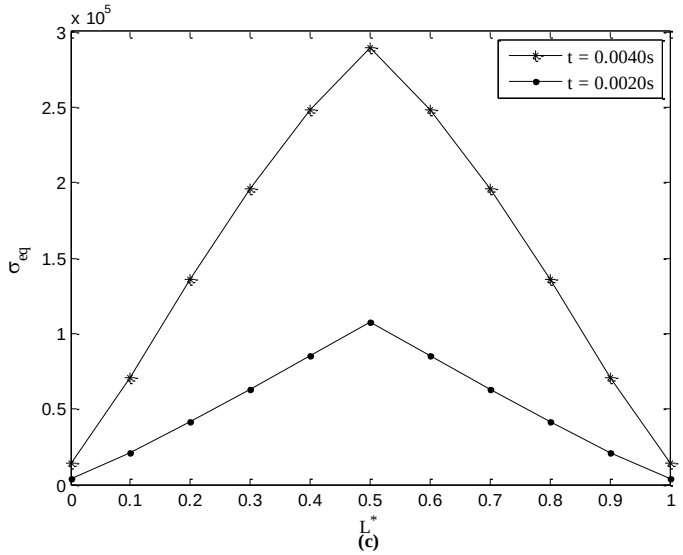

Figure 3.10: Variation of Bending Stress, Shear Stress and Equivalent Stress along the length of rotor

From the equivalent stress plot shown below it can be seen that rotor shaft is highly stressed at its mid-point, hence center of the shaft length is taken as design point for the further analysis.

Rotor shaft is designed on the basis of fatigue analysis. For this purpose endurance strength, is calculated with Goodman relation for assumed value of factor of safety $F_s = 1.5$, failure stress is also interpolated through Goodman diagram on the basis of maximum stress develop at mid-point. Thereafter life corresponding to this failure stress is evaluated through Wohler diagram. Life is defined as the number of cycles that a mechanical component can complete before the appearance of the first fatigue crack over its surface.

It can be seen from the fatigue results in Table 3.4 that failure stress σ_f comes out to be less than the endurance strength σ_e hence design parameters of rotor operation are safe as stress are within safe limit of operation.

Endurance Strength σ_e (MPa)	**Failure Stress** σ_f (MPa)	**Life** N_f (Cycles)
110	74	5.0848×10^6

Table 3.4: Fatigue Analysis Results

For steel if life for the system lies in the range 10^6 to 10^7 which can be taken as infinite, as from the Wohler diagram in fig. 3.3 it can be deduced that when life comes out to be greater than 10^6 cycles then it lies in the region of high cycle fatigue and component has an infinite life. Therefore our results are in accordance with given theory.

Chapter 4

CONCLUSION AND FUTURE SCOPE

4.1 Conclusion

A literature survey has been carried out to investigate the developments in modelling for beam. It is observed that a huge amount of work has been done in modelling different kind beams such as sandwich beam, etc. and most of them involved the Finite Element Modelling. But it was felt that not much has been done involving determination of stresses that are developed during operation of beams and rotor.

Through this work a finite element modelling of beam is achieved and results are validated for mode shapes of undamped Euler Bernoulli beam by formulating equation of motion for beam. Stresses and strain due to transverse loading which causes bending are determined from time domain solution. This has been done for both undamped and damped model. Damped system is achieved by employing either by augmenting thermodynamic fields (ATF) or anelastic displacement fields (ADF) technique. The stress-strain curve for undamped and damped system are in accordance with the supported theory and thus validates the finite element formulation which is done in matlab.

Modelling of viscoelastic three disc rotor has also been done for validation purpose and further this finite element formulation is utilized for fatigue analysis of single disc rotor which subjected to thermal loading and external torque. In addition to time varying bending stress, shear stress as well as equivalent stress are also determined for various location of the shaft. The equivalent stress shows the centre of the rotor shaft is subjected to maximum stress and indicates failure point or design point. Fatigue analysis has been carried out considering design point and the results shows that the design parameters are safe and rotor shaft has infinite life.

4.2) Future Scope

In this work stresses are function of time response i.e. time domain response has been taken to determine stresses in the system. In future this work can be carried out in modal plane which means modal response can be used instead of time response to determine modal distribution of stresses. We have found out most stressed location as a function of beam length similarly this location can be deduced as a function of mode when analysis is based on modal plane i.e. we will find the highly stressed mode and aiming to control the value of stresses in that particular mode through control theory.

This work has lot of scope in future as using this model more realistic conditions of operation can be achieved by incorporating the effect of stress raiser such as notch, fillet, and keyways, etc. in both beams and rotors. Disc mounted on the shaft is considered as lumped mass and but in future, modelling can be done by taking into account the effect turbine blades which were earlier considered as disc on the shaft. If rotor is considered as turbine then turbulence of steam or water and its effect on fatigue life could be taken into account and there are numerous such conditions and effects which could be considered for future work.

The modelling of present work is based on Euler Bernoulli beam theory which neglects shear deformation of the cross-section thus this model is applicable where slenderness ratio (L/D_R) is near to 15 or long rotor shaft. To make this model suitable for short beams Timoshenko Beam theory can be applied which incorporates shear deformation and thus short beams as well as long beams can be analysed through this model.

As there is a great demand of high strength to weight ratio, therefore stress analysis of fibre reinforced composite shaft made of either unidirectional fibre or bidirectional fibres. Manufacturing of rotor using composites becomes economical and is resistant to atmospheric conditions.

4.3) References

1] Slaymaker.R.R., "Mechanical Design and Analysis'', John Willey & Sons, 1959.

2] Bernard J. Hamrock. and Jacobson Bo. and Steven R.Schmid., "Fundamentals of Machine Element'', McGraw-Hill Higher Education, 2004.

3] Khurmi R.S. and Gupta J.K., "Machine Design'', S. Chand Publishers, 2009.

4] Bhandari V.B., "Design of Machine Elements'', Tata McGraw-Hill Education, 2010.

5] Norton R.L., "Machine Design-An Integrated Approach'', Pearson Education, 2003.

6] Jeffcott, H., "The lateral vibration of loaded shafts in the neighbourhood of a whirling speed-the effect of want of balance", Phil. Mag., 37 (6), pp. 304-314, 1919.

7] Nelson H.D. and McVaugh J.N., "The Dynamics of Rotor-Bearing System using Finite Elements", Journal of Engineering for Industry, vol. 98, pp. 593-600, 1976.

8] Zorzi E.S. and Nelson H.D., "Finite Element Simulation of Rotor-Bearing Systems with Internal Damping", Journal of Engineering for Power, Transactions of the ASME, vol. 99, pp. 71-76, 1977.

9] Gujar R.A. and Bhaskar S.V., "Shaft Design under Fatigue Loading by Using Modified Goodman Method", International Journal of Engineering Research and Applications, vol. 3(4), pp.1061-1066, 2013.

10] Goksenli A. and Eryurek I.B., "Failure analysis of an elevator drive shaft", Journal of Engineering Failure Analysis, vol. 16, pp. 1011–1019, 2009.

11] Raotole L. Mahesh, Sadaphale D. B., Chaudhari J. R., "Prediction of Fatigue Life of Crank Shaft using S-N Approach", International Journal of Emerging Technology and Advanced Engineering, Volume 3, Issue 2, February 2013.

12] Jani Romanoff. and Petri Varsta and Alan Klanac., "Stress Analysis of Homogenized Web-Core Sand Sandwich Beams', Journal of composite structure 79 pp 411-4222, 2007.

13] Onur Sayman, Umran Esendemir., "An elastic–plastic stress analysis of simply supported metal-matrix composite beams under a transverse uniformly distributed load", Journal of composite science and technology 62 pp 265-273, 2002.

14] Dutt J.K. and Nakra B. C., "Stability of rotor systems with viscoelastic supports", Journal of Sound and Vibration, 153 (1), pp. 89-96.

15] Roy H., Dutt J. K. and Datta P. K., "The Dynamics of Multi-layered Viscoelastic Beams", Journal of Structural Engineering and Mechanics, vol. 33, pp 391-406, 2009.

16] Muszynska A. "Forward and Backward Precession of a Vertical Anistropically Supported Rotor", Journal of Sound and Vibration, vol 192(1), pp 207-222, 1996.

17] Bauchau O.A.,Craig J.I., **"**Euler-Bernoulli beam theory**",** Journal of Solid Mechanics and its application, Volume 163, pp 173-221, 2009.

18] Lalanne M. and Ferraris G., "Rotor Dynamics Prediction in Engineering", John Wiley and Sons, 1998.

19] Ogata K., "Modern Control Engineering", Pearson Education International, 2002.

20] Zhenxing Shen. and Qiang Tian. and Xiaoning Liu. and Gengkai Hu., "Thermally induced vibrations of flexible beams using Absolute Nodal Coordinate Formulation", Journal of Aerospace Science and Technology 29 pp 386-393, 2013.

21] Narasimha Marakala. and Appu K.K. and Ravikiran Kadoli., "Thermally induced vibration Of a simply supported beam using finite element method", International Journal of Engineering Science and Technology vol 2 (12), pp 7874-7879, 2009.

22] Robert D. Cook, Davis S.M., Michael E.P. and Robert J.W., " Concept And Application of Finite Element Analysis", John Wiley & Sons,2002 4th edition.

23] Genta Giancarlo., Dynamics of rotating systems, Springer Verlag, 2009.

24] Gunter Edgar J. Jr., "Rotor bearing stability", Proceedings of the First Turbo-Machinery Symposium.

25] Zorzi E.S. and Nelson H.D. “The dynamics of rotor-bearing systems with axial torque - A Finite Element Approach”. Journal of Mechanical Design, vol. 102, pp158-61, 1988.

26] Roy H. and Dutt J. K. and Datta P. K., “Dynamics of Viscoelastic Rotor Shaft Using Augmenting Thermodynamics Fields- A Finite Element Approach”, International Journal of Mechanical Science, vol. 50, pp 845-853,2008.

4.5 Appendix

Translatory Mass Matrix $[M_T]$

$$[M_T] = \frac{\rho \times \mathrm{A} \times l_e}{420} \times \begin{bmatrix} 156 & 22l_e & 0 & 0 & 54 & -13l_e & 0 & 0 \\ & 4l_e^2 & 0 & 0 & 13l_e & -3l_e^2 & 0 & 0 \\ & & 156 & -22l_e^2 & 0 & 0 & 54 & 13l_e \\ & & & 4l_e^2 & 0 & 0 & -13l_e & -3l_e^2 \\ & SYMMETRIC & & & 156 & -22l_e & 0 & 0 \\ & & & & & 4l_e^2 & 0 & 0 \\ & & & & & & 156 & 22l_e \\ & & & & & & & 4l_e^2 \end{bmatrix}$$

Rotary Mass Matrix $[M_R]$

$$[M_R] = \frac{\rho \times \mathrm{I}}{30 \times l_e} \times \begin{bmatrix} 36 & 3l_e & 0 & 0 & -36 & 3l_e & 0 & 0 \\ & 4l_e^2 & 0 & 0 & -3l_e & -l_e^2 & 0 & 0 \\ & & 36 & -3l_e^2 & 0 & 0 & -36 & -3l_e \\ & & & 4l_e^2 & 0 & 0 & 3l_e & -l_e^2 \\ & SYMMETRIC & & & 36 & -3l_e & 0 & 0 \\ & & & & & 4l_e^2 & 0 & 0 \\ & & & & & & 36 & 3l_e \\ & & & & & & & 4l_e^2 \end{bmatrix}$$

Bending Stiffness Matrix $\left[K_B\right]$

$$\left[K_B\right]=\frac{E\times \mathrm{I}}{l_e^{\,3}}\times\begin{bmatrix} 12 & 4l_e^{\,2} & 0 & 0 & -12 & 6l_e & 0 & 0 \\ & 4l_e^{\,2} & 0 & 0 & -6l_e & 2l_e^{\,2} & 0 & 0 \\ & & 12 & -6l_e & 0 & 0 & -12 & -6l_e \\ & & & 4l_e^{\,2} & 0 & 0 & 6l_e & 2l_e^{\,2} \\ & SYMMETRIC & & & 12 & -6l_e & 0 & 0 \\ & & & & & 4l_e^{\,2} & 0 & 0 \\ & & & & & & 12 & 6l_e \\ & & & & & & & 4l_e^{\,2} \end{bmatrix}$$

Skew Symmetric Circulatory Matrix $\left[K_C\right]$

$$\left[K_C\right]=\frac{E\times \mathrm{I}}{l_e^{\,3}}\times\begin{bmatrix} 0 & 0 & 12 & -6l_e & 0 & 0 & -12 & -6l_e \\ & 0 & 6l_e & -4l_e^{\,2} & 0 & 0 & -6l_e & -2l_e^{\,2} \\ & & 0 & 0 & 12 & -6l_e & 0 & 0 \\ & SKEW & & 0 & -6l_e & 2l_e^{\,2} & 0 & 0 \\ & SYMMETRIC & & & 0 & 0 & 12 & 6l_e \\ & & & & & 0 & -6l_e & -4l_e^{\,2} \\ & & & & & & 0 & 0 \\ & & & & & & & 0 \end{bmatrix}$$

Gyroscopic and Stiffness Matrices $\left[G\right]$

$$\left[G\right]=\frac{2\times\rho\times\Omega\times \mathrm{I}}{30\times l_e}\times\begin{bmatrix} 0 & 0 & 36 & -3l_e & 0 & 0 & -36 & -3l_e \\ & 0 & 3l_e & -4l_e^{\,2} & 0 & 0 & -3l_e & l_e^{\,2} \\ & & 0 & 0 & 36 & -3l_e & 0 & 0 \\ & SKEW & & 0 & -3l_e & -l_e^{\,2} & 0 & 0 \\ & SYMMETRIC & & & 0 & 0 & 36 & 3l_e \\ & & & & & 0 & -3l_e & -4l_e^{\,2} \\ & & & & & & 0 & 0 \\ & & & & & & & 0 \end{bmatrix}$$

Axial Stiffness Matrix $[K_A]$

$$[K_A] = \frac{P_A}{30 \times l_e} \times \begin{bmatrix} 36 & 3l_e & 0 & 0 & -36 & 3l_e & 0 & 0 \\ & 4l_e^2 & 0 & 0 & -3l_e & -l_e^2 & 0 & 0 \\ & & 36 & -3l_e^2 & 0 & 0 & -36 & -3l_e \\ & & & 4l_e^2 & 0 & 0 & 3l_e & -l_e^2 \\ & SYMMETRIC & & & 36 & -3l_e & 0 & 0 \\ & & & & & 4l_e^2 & 0 & 0 \\ & & & & & & 36 & 3l_e \\ & & & & & & & 4l_e^2 \end{bmatrix}$$

Axial Torque Matrix $[K_T]$

$$[K_T] = T_R \times \begin{bmatrix} 0 & 0 & 0 & \frac{1}{l_e} & 0 & 0 & 0 & -\frac{1}{l_e} \\ 0 & 0 & \frac{1}{l_e} & \frac{1}{2} & 0 & 0 & -\frac{1}{l_e} & -\frac{1}{2} \\ 0 & \frac{1}{l_e} & 0 & 0 & 0 & -\frac{1}{l_e} & 0 & 0 \\ \frac{1}{l_e} & -\frac{1}{2} & 0 & 0 & -\frac{1}{l_e} & \frac{1}{2} & 0 & 0 \\ 0 & 0 & 0 & -\frac{1}{l_e} & 0 & 0 & 0 & \frac{1}{l_e} \\ 0 & 0 & -\frac{1}{l_e} & \frac{1}{2} & 0 & 0 & \frac{1}{l_e} & -\frac{1}{2} \\ 0 & -\frac{1}{l_e} & 0 & 0 & 0 & \frac{1}{l_e} & 0 & 0 \\ -\frac{1}{l_e} & -\frac{1}{2} & 0 & 0 & \frac{1}{l_e} & \frac{1}{2} & 0 & 0 \end{bmatrix}$$